

# Antifungal Films Produced by Polyvinyl Alcohol and Pimaricin with Golden Berry Husk Extract to Extend its Shelf Life

<sup>1</sup>Maha, M. Gomaa, <sup>2</sup>Mohamed, A. Salama & <sup>\*3</sup>Mohamed, E. Abdin

<sup>1</sup>Department of Horticultural Crops Technology Research, Food Technology Research Institute, Agricultural Research Center, Giza, Egypt

<sup>2</sup>Oils and Fats Research Department, Food Technology Research Institute, Agricultural Research Center, Giza, Egypt

<sup>\*3</sup>Food Engineering and Packaging Department, Food Technology Research Institute, Agricultural Research Center, Giza, Egypt

## Original Article

### Article information

Received 15/03/2024

Revised 30/03/2024

Accepted 31/03/2024

Published 31/03/2024

Available online

31/03/2024

### Keywords:

Golden berry; Golden berry husk extract; Food packaging; Antifungal activity; Shelf life preservation

## ABSTRACT

This study investigated the incorporation of golden berry husk extract (HE) into polyvinyl alcohol (PVA) films for food packaging, with a focus on preserving golden berry fruits. Analysis of HE revealed the presence of potent antioxidants such as ferulic acid, quercetin, chlorogenic acid, rutin, and gallic acid. Scanning electron microscopy (SEM) showed increased surface roughness and crack formation in PVA/HE films with higher HE concentrations, indicating favorable interactions between HE phenolic molecules and the PVA matrix. Fourier-transform infrared spectroscopy (FT-IR) confirmed physical interactions between PVA and HE without chemical alterations. Mechanical tests revealed elevated tensile strength and elongation at break for PVA/HE films, suggesting improved flexibility and strength. Water contact angle (WCA) measurements indicated altered hydrophilicity and hydrophobicity with HE incorporation, showing decreased WCA at higher HE concentrations. Increasing HE concentration was correlated with heightened antioxidant activity, with PVA/HE films displaying superior scavenging activity for ABTS and DPPH radicals. Physical properties such as thickness, solubility, swelling degree, moisture content, and water vapor permeability were influenced by HE concentration, exhibiting optimal properties at specific concentrations. Antifungal assays demonstrated inhibition of *Aspergillus niger* and *Aspergillus flavus* growth in PVA/HE films. Application of PVA/HE films on golden berry fruits resulted in reduced weight loss, enhanced pH and total soluble solids (TSS) stability, increased firmness retention, and inhibition of yeast and mold growth compared to uncoated and husk-covered samples. Overall, PVA/HE films hold promise as sustainable packaging materials for extending the shelf life and preserving the quality of perishable food products like golden berries.

## 1. Introduction

Food packaging plays a vital role in preserving and safeguarding food products. However, conventional packaging materials are predominantly composed of synthetic polymers derived from non-renewable resources, contributing significantly to environmental concerns. This has driven a surge in research efforts focused

on developing sustainable food packaging solutions utilizing biopolymers (Cazón et al., 2017). The widespread adoption of synthetic polymers in packaging can be attributed to their advantageous properties, including their formability, cost-effectiveness, suitability for printing, and exceptional resistance to a wide range of environmental and mechanical stresses.

Nonetheless, such packaging materials are environmentally burdensome due to their prolonged degradation time and the potential risk of chemical release, which can compromise food quality (Horodytska et al., 2018). Nowadays, proteins, lipids, and polysaccharides -biopolymers generated from natural sources - are widely used as foundational materials for biodegradable packaging solutions. These materials are recyclable, break down quickly, are non-toxic, and are beneficial to the environment (Talukder et al., 2020; Yao et al., 2020). The food sector, alongside various other industries, has emerged as a significant leader in research efforts aimed at partially or completely replacing traditional materials. Global food waste amounts to over 1.3 billion tons year, according to the Food and Agricultural Organization (FAO) (Gheorghita et al., 2020). It's important to recognize that these sources of pollution encompass residential, commercial, industrial, and agricultural waste. Residual traces of previously contained food products, along with various biomolecules, can often be found on used food packaging. Polyvinyl alcohol (PVA), a synthetic polymer, presents significant potential for the development of bioplastics due to its advantageous properties. One of its notable characteristics is its ability to dissolve in water and biodegrade, making it environmentally friendly. Also, PVA exhibits excellent resistance to oil and chemicals, adding to its desirability as a bioplastic material. Notably, it has demonstrated remarkable stability when exposed to various organic solvents. Due to these properties, PVA finds widespread use in applications such as paper adhesives and packaging materials, making it a versatile and well-suited material for various purposes (Abral et al., 2020; Premkumar, 2019). Active packaging stands out as a highly progressive technology employed to maintain food quality by emitting active substances from the packaging itself. This technology allows for the controlled release of these substances over an extended period, thereby preserving or enhancing the shelf quality and lifespan of the product without directly introducing any materials into the food (Ahmed et al., 2017). Numerous active agents, including anti-

oxidants and antimicrobial substances, can be integrated into packaging materials. This incorporation aims to extend the shelf life of food products, consequently decreasing food waste (Davachi and Shekarabi, 2018; Fabra et al., 2018). By integrating antibacterial agents into biodegradable films, it is possible to enhance the release and efficacy of these agents. The incorporation of food-grade antimicrobial compounds into packaging films has demonstrated improved effectiveness against a broad range of bacteria, including both gram-positive and gram-negative strains (Padgett et al., 1998). Pimaricin is an FDA-approved food additive with GRAS status, known for its powerful antifungal properties and commonly used for cheese preservation. However, natamycin faces challenges due to its poor water solubility and uneven dispersion when applied to food surfaces, potentially diminishing its antifungal effectiveness and leading to high residues in certain areas. Additionally, the instability of the compound when exposed to light and its degradation over extended periods of storage may further weaken its preservative capabilities. Top of Form Despite these limitations, ongoing research aims to improve natamycin's solubility, dispersion, and stability, ensuring its safe and efficient use as a food preservative (Fang et al., 2023; Meena et al., 2021). Polyphenols, being nonvolatile substances, can serve as substitutes for other natural preservatives. Besides their biological functions, natural phenolic compounds are capable of enhancing the physicochemical and functional attributes of edible films. They do this by creating cross-links among biopolymers like polysaccharides and/or proteins, in addition to providing antioxidant properties (Norajit et al., 2010). Lately, there has been a growing interest in natural antioxidants as alternatives to synthetic additives in the food sector. Specifically, extracts from berries, including black chokeberry, blackberry, and cranberry, have been explored for creating films with antioxidant properties. The fruit known as *P. peruviana*, goldenberry, or cape gooseberry, is a climacteric berry with a yellow-orange waxy skin and juicy pulp. It is characterized by its papery husk (calyx) that protects the fruit and contains

approximately 150 to 300 small seeds. This fruit is closely related to the tomatillo and belongs to the Solanaceae plant family, which includes other edible plants like tomatoes, eggplants, and potatoes. The ripe fruit is bright yellow to orange in color and has a mildly tart grape-like flavor. It is often used in various applications, including as an ingredient in paper adhesives and packaging materials. The fruit's unique characteristics and versatility make it a popular choice in culinary and commercial settings (Fischer et al., 2011). The objective of this study was to develop an antifungal packaging system based on PVA incorporated with goldenberry husk extract (HE) and evaluate its impact on the shelf life of goldenberry fruits (GB) during the ripening stage and under commercial storage conditions.

## 2. Materials and Methods

### Materials

Fresh goldenberry fruits for the study were bought from a nearby Kafrelshiekh, Egypt market. The fruit wrappers were from Shoman Plastic Factory, which is located close to El Dakahlia in Egypt. Polyvinyl alcohol (PVA) CAS No: 9002-89-5 with a purity of 94%, viscosity of 22–30 cp, and hydrolysis of 99–99.9 (mole%) was used in the investigation. The two radicals came from Sigma Aldrich Co., Ltd. in St. Louis, MO, USA: DPPH and ABTS. Additionally, glycerol plasticizer and pimaricin were bought from Gamma Scientific Company in Egypt. Both fungal strains of *Aspergillus niger* ATCC 6275 and *Aspergillus flavus* ATCC 9643 were purchased from Mericen at Ain Shams University.

### Methods

#### Preparation of golden berry husk extract (HE)

Twenty grams of dried golden berry husk were pulverized and then subjected to extraction using 70% ethanol (200 mL) at ambient temperature (22 °C) for 48 hours. This extraction procedure was performed twice, and the resultant extracts were passed through a filter. A rotary evaporator was then used to concentrate the liquid that had been filtered. At -80 °C, the condensed extract was subsequently fro-

zen. The golden berry extract underwent a 48-hour freeze-drying process at -40 °C to create a lyophilized powder. After that, the lyophilized powder was kept in storage at -20 °C until HE was required.

#### Characterization of GBE

The quantification of GBE bioactive compounds was achieved through the use of an LC-ESI-QTOFMS setup (G2-XS QTOF, Waters, Manchester, UK), adapting a method previously outlined (Eltabakh et al., 2021) with necessary adjustments. In summary, GBE samples were diluted to a concentration of 2 mg/mL and then subjected to centrifugation at 5000 rpm for 20 minutes at a temperature of 30 °C. The supernatant was collected, and aliquots of 1.5 mL were transferred into HPLC vials for subsequent LC-MS analysis. For chromatographic separation, 2 µL of the extract was introduced into an ACQUITY UPLC BEH C18 column (2.1×100 mm), maintaining a flow rate of 0.4 mL/min. The mobile phase consisted of 0.4% formic acid for the initial phase and 0.3% formic acid in acetonitrile for the secondary phase. Mass spectra were generated using an electrospray ionization source operating in positive mode, spanning a mass range of 100 to 1600 m/z, with the ion source temperature set at 800 °C and an ionization voltage of 2.5 kV. Analysis and data processing were conducted using MassLynx software version 4.1.

#### Manufacturing process of polyvinyl alcohol (PVA) and HE films

A weight of 3 g of PVA was mixed at 900 rpm in 100 mL of distilled water at a temperature of 95 °C for 30 min. Subsequently, 0.7 g of glycerol was incorporated as a plasticizer and an additional stirring time of 20 min was followed. After cooling the mixture, varying amounts of freeze-dried HE (0.2, 0.4, and 0.6 g) were introduced to the PVA mixture with an equal amount of pimaricin (100 mg) to form PVA/HE1, PVA/HE2 and PVA/HE3 mixtures, respectively. These were then mixed at 900 rpm with the initial solution for an additional 30 minutes at 45 °C. The final mixture was then evenly distributed onto specialized glass plates measuring 20 cm by 30 cm and allowed to dry for 6 hours at 40 °C. Once dry, the films were gently removed,

and stored in a desiccator, separated by paper sheets for later analysis. The PVA films were prepared with the same methodology without adding pimaricin or HE.

### SEM analysis

Observations of surface imperfections, such as cracks or wrinkles, on the film samples were carried out using an SEM (Scanning Electron Microscope, model SU8010, Hitachi, Japan). Samples of the films were trimmed into square shapes measuring 10 × 10 mm and then mounted onto aluminum stubs as a preparatory step before being coated with a thin layer of gold to enhance the surface's conductivity. The SEM images were taken at an appropriate magnification level to allow for a detailed examination of the film's surface texture.

### FTIR analysis

The wavelength spectra of the samples were documented using a Nicolet iS-50 FT-IR spectrometer (Thermo Fisher Scientific, USA), spanning a range from 4000 to 500 cm<sup>-1</sup> (Abdin et al., 2021).

### Differential Scanning Calorimetry analysis of films

Differential scanning calorimetry (DSC) analysis was performed using a Shimadzu DSC-60 Plus instrument. Accurately weighed 3 mg samples of the films were placed in aluminum pans and sealed hermetically with a crimping press. These pans were then loaded into the designated sample holders of the instrument, with empty pans serving as references in the opposing positions. The temperature program was set to heat the samples from 0 °C to 400 °C at a constant ramp rate of 10 °C/min.

### Mechanical properties

The mechanical properties of the films were evaluated by measuring their tensile strength (TS) and elongation at break (EB) using a texture analyzer (TA.XT Plus, Stable Micro Systems Ltd., Surrey, UK). Rectangular film samples (20 mm x 100 mm) were secured between the upper and lower grips of the analyzer. A tensile test was conduct-

ed at a crosshead speed of 100 mm/min with a constant force of 100 N. Stress-strain data collected during the test was analyzed using Zwick software (Test Expert V11.02).

### Determination of water contact angle (WCA) of films

The WCA of films was measured according to (Kraisit et al., 2015) with suitable modifications. The wettability of the film surfaces was assessed using the water contact angle (WCA) method. Briefly, each sample was secured to a glass slide with double-sided adhesive tape. A deionized water droplet (volume typically between 3-5 µL) was dispensed onto the film surface using a micropipette. The droplet profile was then captured and analyzed using a goniometer to determine the WCA. This procedure was replicated four times per sample for statistical significance. The WCA values provide valuable information regarding the surface hydrophobicity/hydrophilicity of the films.

### Determination of antioxidant activity of films

#### DPPH and ABTS activity

The antioxidant capacity of the films was assessed by evaluating their ability to neutralize DPPH and ABTS radicals. For the DPPH radical scavenging activity, the procedure outlined by (Siripatrawan and Harte, 2010) was followed with minor modifications. Initially, 100 mg of film samples were soaked in 10 mL of 10% (v/v) methanol and agitated at 120 rpm for 3 hours. Following this, the samples were centrifuged to separate the supernatant. Subsequently, 0.5 mL of each supernatant was combined with 4.5 mL of a methanolic DPPH solution (1 mM) that had been prepared in advance. To initiate the reaction, the mixture was thoroughly vortexed for 30 minutes, and the absorbance was measured at 517 nm both before and after the addition of the sample. The resulting data were then analyzed using a specific equation to determine the scavenging activity.

$$\text{DPPH radical scavenging activity (\%)} = \left( \frac{\text{Ab of DPPH} - \text{Ab of tested sample}}{\text{Ab of DPPH}} \right) \times 100$$



The ABTS radical scavenging capacity of the films was evaluated using a modified version of the method described by (Kim et al., 2018). Briefly, a radical cation solution was prepared by mixing 145 mM potassium persulfate and 7 mM 2,2'-Azino-bis(3-ethylbenzothiazoline-6-sulfonic acid) (ABTS) solution in a 1:1 ratio. This mixture was incubated in the dark for 12 hours to ensure complete ABTS radical formation. The solution was then diluted with phos-

phate-buffered saline (PBS, 0.2 M, pH 7.4) to achieve an initial absorbance of approximately 0.7-0.8 at 734 nm. Film extracts (20 mL) were then combined with 1980 µL of the diluted ABTS solution. The absorbance of this mixture was measured at 734 nm after a specific incubation time. The percentage inhibition of the ABTS radical was calculated using a standard formula.

$$ABTS \text{ radical scavenging activity (\%)} = \left( 1 - \frac{Abs \text{ film samples} - Abs \text{ film samples with PBS}}{Abs \text{ ABTS}} \right)$$

### Physical properties of films

Film thickness was measured using a digital electronic micrometer. After trimming the films into smaller pieces, each piece was positioned vertically between the micrometer's jaws. Measurements were taken at six locations on each film section, and the average thickness was calculated from these values to represent the film's overall thickness. To assess the moisture percentage and water solubility of films, five 2x2 cm<sup>2</sup> film samples were weighed to obtain their wet weight (M1). The samples were then dried in a hot air oven at 105°C until they reached a constant weight, after which they were weighed again to obtain their dried weight (M2). The moisture content was calculated using the recorded weights.

$$Moisture \text{ content (\%)} = \left( \frac{M1 - M2}{M1} \right) \times 100$$

After drying, the samples were soaked in 30 mL of distilled water for 24 hours. The insoluble film portions were collected by filtering the mixture through pre-weighed filter paper. The filter papers were divided into two groups: one set was re-dried at 105 °C until a constant weight was reached (final weight recorded as M3), while the other set was allowed to air dry at room temperature (final weight recorded as M4). The solubility and swelling degree were then calculated using specific equations:

$$Solubility (\%) = \left( \frac{M2 - M3}{M2} \right) \times 100$$

$$Swelling \text{ degree (\%)} = \left( \frac{M4 - M3}{M3} \right) \times 100$$

To measure the water vapor permeability (WVP) of the films, a conical flask containing 15 mL of distilled water was sealed with the film and placed in a desiccator at 50% relative humidity and 25°C. This setup created a water vapor pressure difference across the film. Using a digital gauge, the pressure differences were monitored, and the weight of the flasks was recorded every 2 hours for 12 hours (Du et al., 2021). The WVP was then calculated using the subsequent equation:

$$WVP = \frac{\Delta w \cdot f}{A \cdot t \cdot \Delta P}$$

Δw= changes in weight of the flasks, f= the thickness of the films, A, the exposed area of films, t, the time interval of every 2 hours, and ΔP, the changes in water pressure between the internal and external sides of the films.

### Antifungal effects of films

The inhibition of *Aspergillus niger* ATCC 6275 or *Aspergillus flavus* ATCC 9643 by films was evaluated using the inhibition zone method (Xu et al., 2023). In this method, a suspension of *Aspergillus niger* or *Aspergillus flavus* with a concentration of 1 × 10<sup>6</sup> CFU/mL was added to the PDA culture medium at a ratio of 1:100 (v/v). The mixture was then poured into culture plates and allowed to solidify. Film disks with a diameter of 9 mm were created in the middle of the culture medium. The plates were incubated at 28°C for 4 days, and the diameter of the inhibition zone was measured using a vernier caliper.

## Application of films on golden berry fruits as packaging material

The golden berry with a number of 10 fruits was sealed between two pieces measuring 25 × 25 cm using double-layer bags made of PVA/HE2 and polyethylene cover (PEC). PVA/HE2 was selected as an ideal package material with satisfied water vapor properties, thickness, mechanical properties, good surface structure and antifungal activity. To seal the bags tightly, a heater impulse sealer machine from Mercier Corporation (model ME-455A1, Taipei, Taiwan) was used. The uncovered fruits (UC) and natural husk-covered fruits (HC) were considered controls for real comprehension. All samples were kept at a temperature of 4 °C for a period of 20 days. At intervals of 5 days, three replicates from each type of bag were taken out for further analysis.

## Characterization of GB fruits during cold storage

### Determination of pH, TSS and reducing sugars

Goldenberry juice samples weighing 24 grams were extracted using a ground blender manufactured by Black & Decker in Colombia. The total soluble solids (TSS) content of the juice was measured using a portable refractometer (PAL-1, ATAGO, Fukaya-shi, Japan) in accordance with the 932.12 AOAC method (AOAC, 1995) and expressed as °Brix. The pH of the juice extract was determined by immersing the electrode of a pH meter (pH Basic+, Sartorius, Gotinga, Germany) into the juice extract. Finally, the reducing sugar content was evaluated using the method reported by (Miller 1959).

### Determination of weight loss and firmness

The percentage of weight loss (WL) for covered and uncovered samples of GB was calculated using the following formula:

$$\text{Weight loss} = 100 \times \left( \frac{W_{\text{zero time}} - W_{\text{final time}}}{W_{\text{zero time}}} \right)$$

Where  $W_{\text{Zero time}}$  = weight at the beginning of the experiment and  $W_{\text{Final time}}$  = the weight at the end of storage time.

Fruit firmness was determined using a texturometer (LS1, Lloyd Instruments Ltd., Largo, FL, USA) equipped with a 1 kN load cell. Individual fruits were centrally positioned on a stable platform. A cylindrical probe (2 mm diameter) was then employed to perform a puncture test at a constant compression speed of 40 mm/min." The reported results represent the average of six repetitions for each treatment.

### Determination of respiratory rate

The respiration rate of golden berries (GB) was assessed using a modified closed system method (Banda et al., 2015). Briefly, 150 g samples of both control and coated GB fruits, previously stored at 8°C, were placed in individual 1 L sealed glass jars. The CO<sub>2</sub> concentration within the headspace of each jar was monitored using a gas analyzer (Checkmate 3, PBI Dansensor, Ringstead, Denmark) at 30-minute intervals over a 3-hour period. The respiration rate was then calculated using a following equation:

$$y_{CO_2} = Y_i CO_2 + \left( \frac{R CO_2 w}{V_f} \right) (t - t_0)$$

In this equation,  $y_{CO_2}$  represents the CO<sub>2</sub> concentration (%) at a specific time (t), while  $y_i CO_2$  represents the CO<sub>2</sub> concentration at the initial time (t<sub>0</sub>). The total weight of the product (W) in kilograms and the free volume inside the glass jar (V<sub>f</sub>) in milliliters were also considered in the calculation.

### Yeast and mold analysis of GB fruits covered with films

Yeast and mold enumeration was performed following a previously established method (Hashemi et al., 2017). Briefly, 10 g of goldenberry samples were homogenized for 2 minutes in 90 mL of sterilized 0.1% (w/v) peptone water. Ten-fold serial dilutions were then prepared using potato dextrose agar (PDA; Oxoid) and dispensed into Petri dishes. The plates were subsequently incubated at 25 °C for 5 days to allow for colony formation.

### Statistical analysis

The statistical analysis used to detect variance in the different properties of GB fruits was conducted using SPSS 20.0 software. The Tukey's honest significant difference (HSD) test was utilized to determine the differences between means. If the p-value was less than 0.05, the differences were considered significant.

### 3. Results and Discussions

#### Characterizations of HE

The following Table 1. displays the outcomes of the chromatographic profile and MS data examina-

tion of eight compounds identified during the experiment. The main compounds that were tentatively identified include ferulic acid, quercetin, chlorogenic acid, rutin, and gallic acid, with concentrations of 44.83, 33.09, 27.16, 22.19, and 18.42  $\mu\text{g/g}$ , respectively, in the dry sample. The presence of rutin, quercetin, and chlorogenic acid was proven previously (Etzbach et al., 2018).

**Table 1. The profile of bioactive components of HE by LC-ESI-QTOF-MS**

Detected compounds	Retention time (min)	MW (Da)	Calibration equation	Regression coefficient R <sup>2</sup>	$\mu\text{g/g}$ of dry sample
Gallic acid	9.79	170.12	$y=8454.12x+3520.3$	0.8501	18.42
Kaempferol	12.87	286.23	$y=6312.72x+3870.3$	0.9890	11.35
Ferulic acid	13.96	194.25	$y=7812.10x+1252.7$	0.9410	44.83
Quercetin	10.05	302.96	$y=6748.73x+6312.3$	0.9521	33.09
Caffeic acid	8.03	180.16	$y=5841.19x+5241.3$	0.9861	8.89
Carvacrol	15.71	150.21	$y=7321.20x+6540.8$	0.9172	15.71
Rutin	14.52	610.07	$y=8821.40x+6512.7$	0.9320	22.19
Chlorogenic acid	10.63	354.37	$y=7541.80x+5721.4$	0.8520	27.16

#### SEM micrographs

The surface morphology of the control PVA film and the PVA/HE film was analyzed using SEM. The control PVA film (Figure 1A) exhibited a rough surface without any visible cracks, indicating that the polymers were well-dispersed and showed compatibility between molecules. On the other hand, the surface of the PVA/HE film with lower concentrations of purified HE (Figure 1B-C) showed some roughness without prominent cracks. This suggests that the inclusion of HE phenolic molecules fostered favorable interaction with the PVA film at lower concentrations. However, when higher concentrations of HE (0.6%) were added to the PVA film, uneven curls and noticeable cracks

formed (Figure 1D). This observation aligns with previous findings (Alshehri et al., 2023).

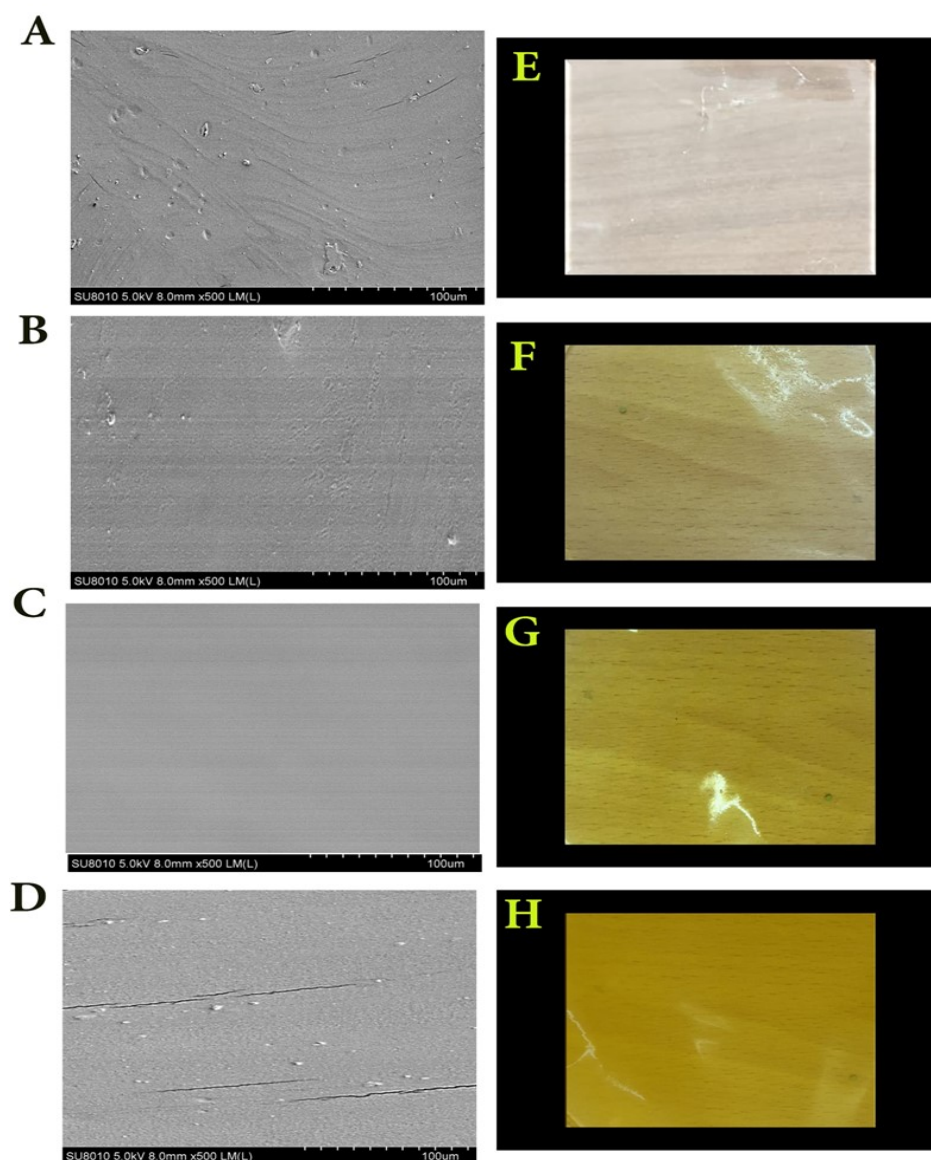


**Figure 1. SEM surface images and real images of PVA (A-E), PVA/HE1 (B-F), PVA/HE2 (C-G) and PVA/HE3 (D-H)**

### FT-IR characterization of PVA/HE films

FT-IR analysis was performed to investigate the interaction between the PVA film matrix and HE (Figure 2A). The FT-IR spectrum of the PVA sample exhibited several characteristic peaks. A broad and strong band centered at  $3265\text{ cm}^{-1}$  indicated the stretching vibration of the hydroxyl group with strong hydrogen bonding. Additionally, a smaller band at  $2810\text{ cm}^{-1}$  was attributed to  $\text{CH}_2$  and  $\text{CH}$  stretching vibrations. The presence of carbonyl functional groups was indicated by a stretching vibrational band observed at  $1595\text{ cm}^{-1}$  in the FT-IR spectrum. The C-O stretching vibration bands at  $1086$  and  $1024\text{ cm}^{-1}$  were identified as bands sensi-

tive to crystallization based on the analysis (Alshehri et al., 2023; Korbag and Mohamed Saleh, 2016). When comparing the FT-IR spectra of PVA films with HE at different concentrations to those of pure PVA film, no discernible alterations were seen (Figure 2A). This implies that HE is incorporated into the PVA matrix without undergoing any chemical changes to its phenolic structure. This change suggests that PVA and HE are physically interacting, which is advantageous since it allows them to share the original active ingredients without compromising their bioactivity. Previous investigations have already confirmed the physical relationship (Gomaa et al., 2022).



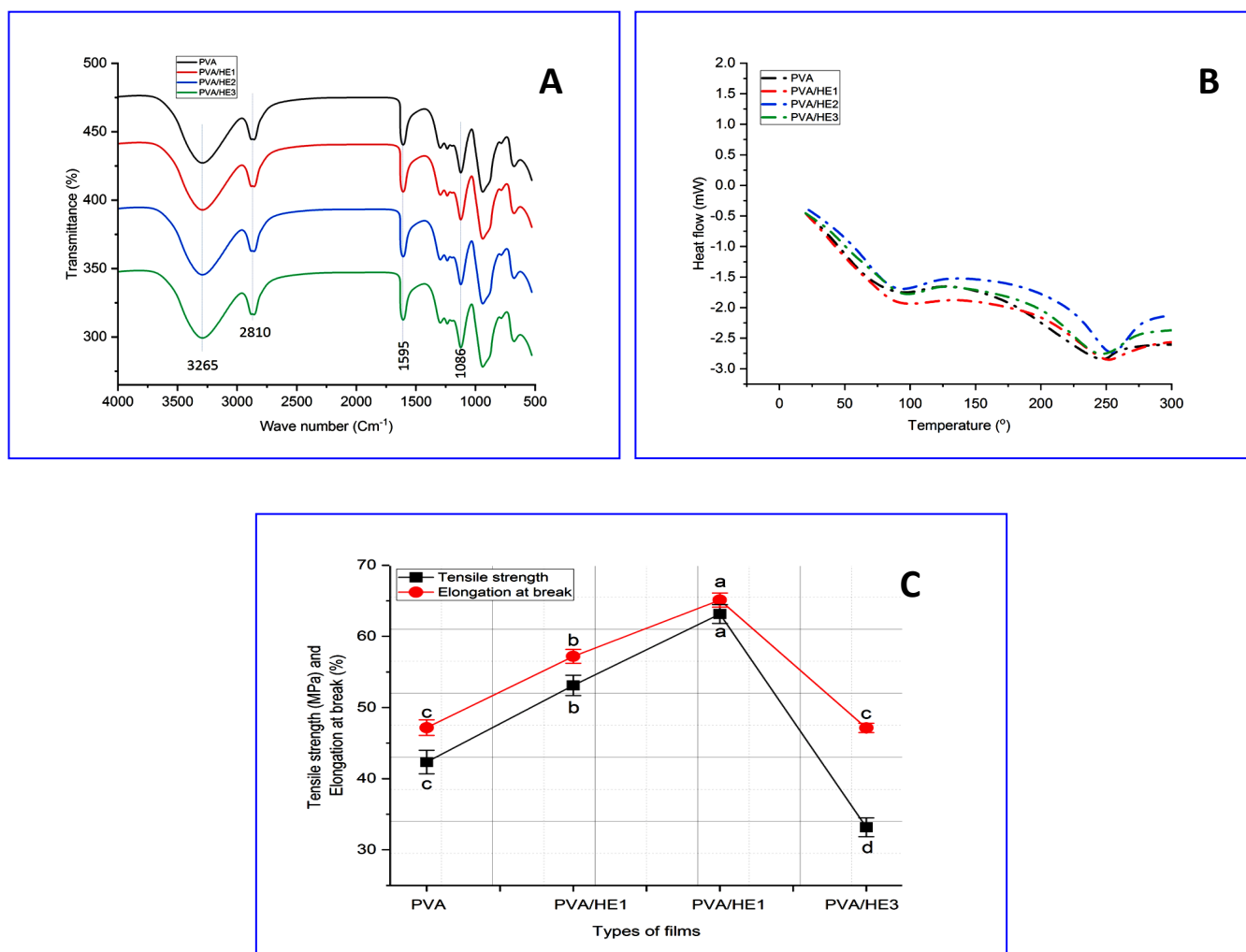


**Figure 2.** FT-IR spectra (A), DSC curves (B) and mechanical properties (C) of PVA/HE films

### Thermal characteristics by DSC analysis

The temperature transition and variations in crystallinity of the treated films were ascertained by DSC. Every sample showed unique endothermic and exothermic curves, as shown in Figure 2B. The water evaporation that resulted from the samples' heat absorption could be the cause of the observed endothermic peak (Su et al., 2010). As the temperature has risen to 225 °C, PVA/HE films have received enough energy to break down, resulting in the development of the second endothermic peak (Martins et al., 2012). Incorporation of HE into the PVA matrix resulted in a shift towards exothermic behavior. The peak exothermic decomposition temperatures for PVA/HE1 and PVA/HE2 were observed at 250.34°C and 254.65°C, respectively. Conversely, the control PVA film exhibited an en-

dothermic peak at around 248.31°C. On the other hand, the PVA/HE3 curve showed a decreasing trend in thermal stability and an exothermic temperature of 247.33 °C. The incorporation of HE into the PVA matrix enhanced the thermal stability of PVA films up to a specific concentration (PVA/HE2), likely due to the inherent heat resistance of the phenolic compounds in HE and the favorable intermolecular interactions between HE and the PVA polymer (Goudarzi et al., 2023). However, at higher HE loadings (PVA/HE3), a decrease in thermal stability was observed. This phenomenon could be attributed to structural disturbances within the PVA matrix, potentially affecting the crystallinity of the film components. This hypothesis aligns with the observations from the subsequent SEM surface analysis (Pankaj et al., 2014).

## Tensile strength and elongation at break of PVA/HE films

The mechanical properties of films can be examined by an analysis of their elongation at break (EB) and tensile strength (TS) characteristics. These variables are thought to be among the most effective ways to assess the elasticity and strength of films. As shown in Fig. 2C, when HE was added, the TS and EB values for PVA/HE1 and PVA/HE2 rose significantly ( $P < 0.05$ ) in comparison to the control (PVA). This phenomenon can be linked to the presence of glycerol and the phenolic components found in the HE chemical structure, which slow down the films' stiffness (Zarandona et al., 2020). Furthermore, the PVA films showed homogeneity in structure, which allows for a strong hydrogen or ionic bond interaction between the hydroxyl groups of the film matrix and the polyphenolic components of the HE. The prior research clarified that the polyphenols from *Cinnamomum camphora* seeds and carboxymethyl chitosan-gum Arabic enhanced TS and EB (Alnadari et al., 2022). After applying high concentrations of HE 0.6% inside PVA/HE3 films, TS and EB characteristics were shown to degrade, with a decrease in TS (33.17%) and EB (47.13%). The internal molecular

force and the structure of the polymer are important factors that affect its mechanical properties (Gomaa et al., 2022). The SEM results proved the presence of cracks that weaken a film's capacity to stretch, which in turn causes a decline in TS and EB.

## Water contact angel (WCA) of PVA/HE films

To determine whether a surface is hydrophilic or hydrophobic, the water contact angle (WCA) is frequently measured. A surface's degree of surface activation can be determined by looking at the angle at which water droplets converge on it. WCA was observed at  $80.31^\circ$  in the PVA films, as shown in Fig. 3A. PVA/HE1 and PVA/HE2 had WCA of  $84.11^\circ$  and  $87.32^\circ$ , respectively, due to the presence of HEE. The WCA value dropped to  $83.32^\circ$  as the HE concentration in PVA rose (PVA/HE3). The observed changes in the films' water contact angle could potentially be explained by the minor increase in roughness that was noted, resulting in a larger specific surface area (Jiang et al., 2021). This observation, together with surface fissures and crack changes as shown by SEM micrographs, may be partially to blame for the drop in WCA in PVA/HE3 films. The same trend was observed previously with (Alshehri et al., 2023).

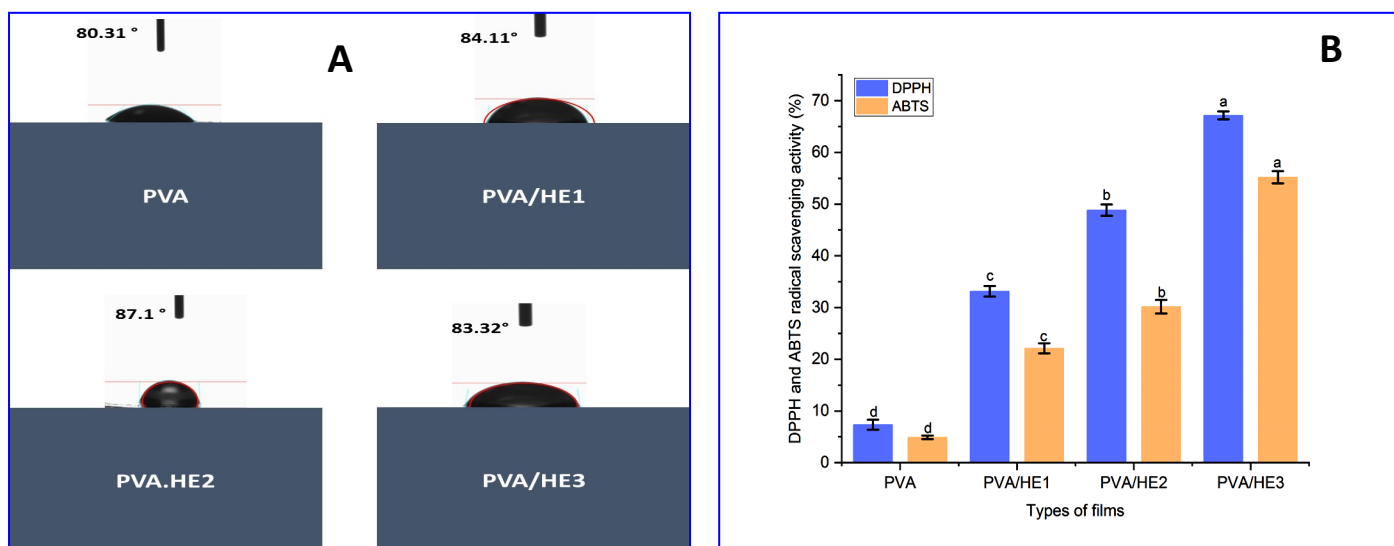


Figure 3. Water contact angel (A) and antioxidant activity (B) of PVA/HE films

### Antioxidant activity of PVA/HE films

Among the samples, PVA/HE3 films displayed the highest free radical scavenging activity, achieving 55.19% and 67.7% inhibition of ABTS and DPPH radicals, respectively (Figure 3B). These films were followed by PVA/HE2 and PVA/HE1 ( $p < 0.05$ ). Thus, it can be said that PVA/HE3 showed the highest scavenging activity for these radicals among the studied film samples. According to the study, the presence of HE extracts is mostly responsible for the film's antioxidant activity. This is probably due to the superior free radical scavenging activity of PVA/HE3 films can likely be attributed to" for a more specific cause-and-effect explanation. (Mittal et al., 2021). One method for increasing food products' shelf life that shows promise and works well is the use of packaging films with enhanced antioxidant activity. The antioxidant activity that results from adding extracts with high hydroxyl group content to the films might help stop or slow down food product oxidation, minimizing spoilage and increasing the packaged goods' shelf life.

### Physical properties of PVA/HE films

This experiment aimed to investigate the influence of active components, such as HE, on the physical properties of PVA/HE films. The study focused on assessing several characteristics of the films, including thickness, swelling degree, solubility, moisture content, and water vapor permeability. According to Table 2., the results indicate that as the concentration of HE increased in PVA/HE films, there was a notable and statistically significant ( $p < 0.05$ ) increase in the thickness of the film. The PVA/HE3 film exhibited the highest thickness (0.182 mm), suggesting a positive correlation between HE content and film thickness. This observation could be attributed to the increased mass introduced during the incorporation of higher HE levels. A plausible hypothesis is that there is a positive relationship between the concentration of polyphenols and the thickness of the film. Large molecules called polyphenols often cluster together to form a network-like structure within the film, giving the impression that the film is thicker (Sogut and Seydim, 2018). The findings in Table 2. demonstrate

that the films' degree of swelling and solubility decreased as the polyphenol concentration in the films rose. PVA/HE3 films displayed the lowest swelling degree (20.71%) and solubility (14.90%). The hydrophobicity of some polyphenols and their ability to form hydrophobic network groups can cause a decrease in solubility and a degree of film swelling. (Alshehri et al., 2023). As the concentration of HE rises, there is a noticeable reduction in the moisture content of the films. This reduction is attributed to the hydrophobic nature of HE functional groups, which repel water. These groups create a barrier within the film, obstructing the penetration of water molecules. Furthermore, the incorporation of HE likely strengthens intermolecular interactions between the phenolic moieties within HE and the hydroxyl/amino groups of the PVA polymer.

This phenomenon can lead to the formation of a more compact and less hydrophilic film matrix, hindering water molecule interactions and consequently reducing the film's water uptake capacity (Chaudhary et al., 2021).

Regarding water vapor permeability (*WVP*), the values for PVA and PVA/HE films are presented in Table 2. The research indicated that the PVA films exhibited a water vapor transfer rate of  $3.2421 (\times 10^{-10} \text{ g.m}^{-1} \text{ s}^{-1} \text{ pa}^{-1})$ . With an increase in HE content from 0.4 to 0.6%, there was a noted reduction in *WVP* for PVA/HE films, decreasing from 3.022 to  $1.431 (\times 10^{-10} \text{ g.m}^{-1} \text{ s}^{-1} \text{ pa}^{-1})$ , a difference that was statistically significant ( $p < 0.05$ ). This trend aligns with prior studies, highlighting that the phenolic constituents in the extracts may form bonds with the polymer chains, thus limiting their interaction with water and consequently diminishing the films' *WVP* (Chaudhary et al., 2021 and Severo et al., 2021). Nevertheless, further increasing the HE content to a concentration of 1.5% led to an elevation in the *WVP* to  $3.003 (\times 10^{-10} \text{ g.m}^{-1} \text{ s}^{-1} \text{ pa}^{-1})$ . This increase in permeability can be attributed to the formation of surface and internal fractures in the films, which were a result of the higher HE concentrations, potentially facilitating the evaporation of water vapor from the films.

**Table 2. Physical properties of PVA films incorporated with HE**

Films samples	Thickness (mm)	Swelling degree (%)	Solubility (%)	Moisture content (%)	WVP ( $\times 10^{-10} \text{ g}\cdot\text{m}^{-1} \text{ s}^{-1} \text{ pa}^{-1}$ )
PVA	0.105 $\pm$ 0.0030 <sup>d</sup>	37.30 $\pm$ 0.16 <sup>a</sup>	27.13 $\pm$ 0.24 <sup>a</sup>	13.29 $\pm$ 0.33 <sup>a</sup>	3.2421 $\pm$ 0.002 <sup>a</sup>
PVA/HE1	0.133 $\pm$ 0.0011 <sup>c</sup>	32.05 $\pm$ 0.22 <sup>b</sup>	20.01 $\pm$ 0.37 <sup>b</sup>	10.01 $\pm$ 0.27 <sup>b</sup>	3.022 $\pm$ 0.001 <sup>b</sup>
PVA/HE2	0.152 $\pm$ 0.0023 <sup>b</sup>	24.33 $\pm$ 0.34 <sup>c</sup>	17.06 $\pm$ 0.41 <sup>c</sup>	7.99 $\pm$ 0.10 <sup>c</sup>	1.431 $\pm$ 0.004 <sup>c</sup>
PVA/HE3	0.182 $\pm$ 0.0043 <sup>a</sup>	20.71 $\pm$ 0.81 <sup>d</sup>	14.90 $\pm$ 0.33 <sup>d</sup>	5.01 $\pm$ 0.04 <sup>d</sup>	3.003 $\pm$ 0.003 <sup>b</sup>

Values are presented as mean  $\pm$  standard deviation. Different letters (a–d) in the similar column show significant differences ( $p < 0.05$ ) between samples. PVA=polyvinyl alcohol films, PVA/HE1= polyvinyl alcohol with first concentration of husk extract, PVA/HE2 = polyvinyl alcohol with second concentration of husk extract and PVA/HE3 = polyvinyl alcohol with third concentration of husk extract

### Antifungal activity of PVA/HE films

The antifungal efficacy of the films was evaluated by observing their impact on the growth of *Aspergillus niger* and *Aspergillus flavus* using the disk diffusion method (Figure 4A-D). It was observed that the PVA films did not exhibit any inhibitory effect, as there was no discernible zone of inhibition around the film disk in both fungus strains. In contrast, the PVA/HE1-3 films demonstrated a substantial zone of inhibition with an increasing rate on both fungal strains by increasing the concentration of HE. The addition of pimaricin besides the functional HE could cause a synergistic effect on the inhibition of fungal strains. The antifungal activity of pimaricin stems from its ability to target ergosterol, a crucial sterol component of fungal cell membranes. Pimaricin specifically binds to ergosterol, thereby disrupting essential cellular processes such as vacuole fusion, which are reliant on ergosterol's structural integrity. Additionally, this binding also interferes with membrane fusion and fission processes in the fungal cells, impeding their growth and development (Cao et al., 2023). Additionally, the HE, which contains ferulic acid with a satisfactory percentage (Table 1), could help in the inhibition of fungal growth. Ferulic acid was proven to inhibit fungal growth through the formation of a coarse surface with wrinkles, blurry ultrastructure edges, and cytoplasmic leakage on the hyphae cell membrane (Yan et al., 2023). Previous studies proved that the presence of natamycin inside carboxymethyl cellulose packaging coating material improved the antibacterial effect on the surface of

mozzarella cheese (Azhdari and Moradi, 2022).

### Application to golden berry fruits

The weight loss of golden berries (GB) stored under various packaging conditions (Figure 5A) is compared to the weight loss of GB in unpackaged control (UC) samples. The loss of weight in GB is mainly caused by the loss of water, which leads to several changes, including mechanical, textural, visual, and chemical alterations. These changes ultimately result in a decline in the quality of GB and lead to a shortened shelf life. Consequently, addressing this challenge is crucial in order to successfully commercialize GB and ensure its quality and longevity (Rahul Thakur et al., 2019). The UC samples of golden berry (GB) exhibited the highest percentage of weight loss during cold storage time, as indicated in the study.

On the other hand, GB samples packaged with PVA/HE3 showed stability in weight loss throughout the storage period. However, samples packaged with PEC showed a similar increasing trend in GB weight loss during storage time. The combination of PVA with HE in the packaging material demonstrated the ability to regulate gas exchange, water evaporation, and solute migration while also inhibiting fungal growth that could consume GB components and contribute to increased weight loss. These findings align with previous research (Licodiedoff et al., 2016), which utilized gelatin-calcium chloride solution films for maintaining the quality of GB fruits. Figure 5B-C also presents the pH, TSS, and firmness values for both UC and packaged GB during cold storage.



The GB fruits that were coated with PVA/HE2 exhibited pH stability, with no significant differences observed until the 10th day of storage. However, after that point, the pH values gradually increased at a slower rate. In comparison, the GB fruits covered with PEC exhibited the highest pH values (5.12) after 20 days of storage. The uncoated (UC) samples recorded a pH value of 4.87. The fruits covered with PVA/HE3 showed similar patterns to those coated with PEC, with no significant differences in pH values observed until 10 days of storage. However, after 10 days, the pH values increased. The increase in pH during post-harvest storage reflects the degradation of starch and the consumption of organic acids through the respiration process. This suggests that the PVA/HE3 films did not influence the biochemical processes associated with these pa-

rameters in goldenberries (Thakur et al., 2018). Regarding the TSS (Figure 5C), an overall increase in TSS values from day 0 to day 10 was observed, which can be attributed to the hydrolysis process converting starch into simple sugars. However, after 10 days of storage, a significant reduction in TSS values was observed in UC, HC, and PEC-covered samples compared with PVA/HE2-covered samples. This reduction in TSS values in UC, HC, and PEC samples may be attributed to the consumption of organic acids and sugars during the respiratory process (Galindez et al., 2021). This consumption occurred at a higher rate in UC, HC, and PEC samples compared to the PVA/HE2-covered samples. The findings demonstrate that PVA/HE2 films effectively reduced the respiration rate of GB fruits.

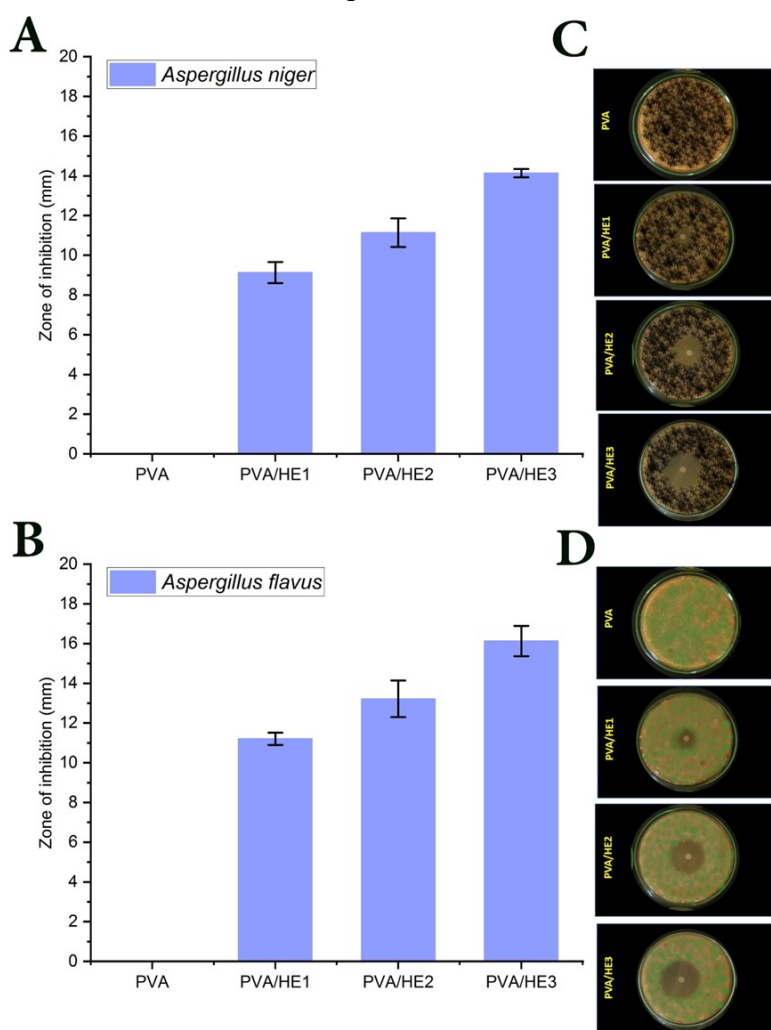
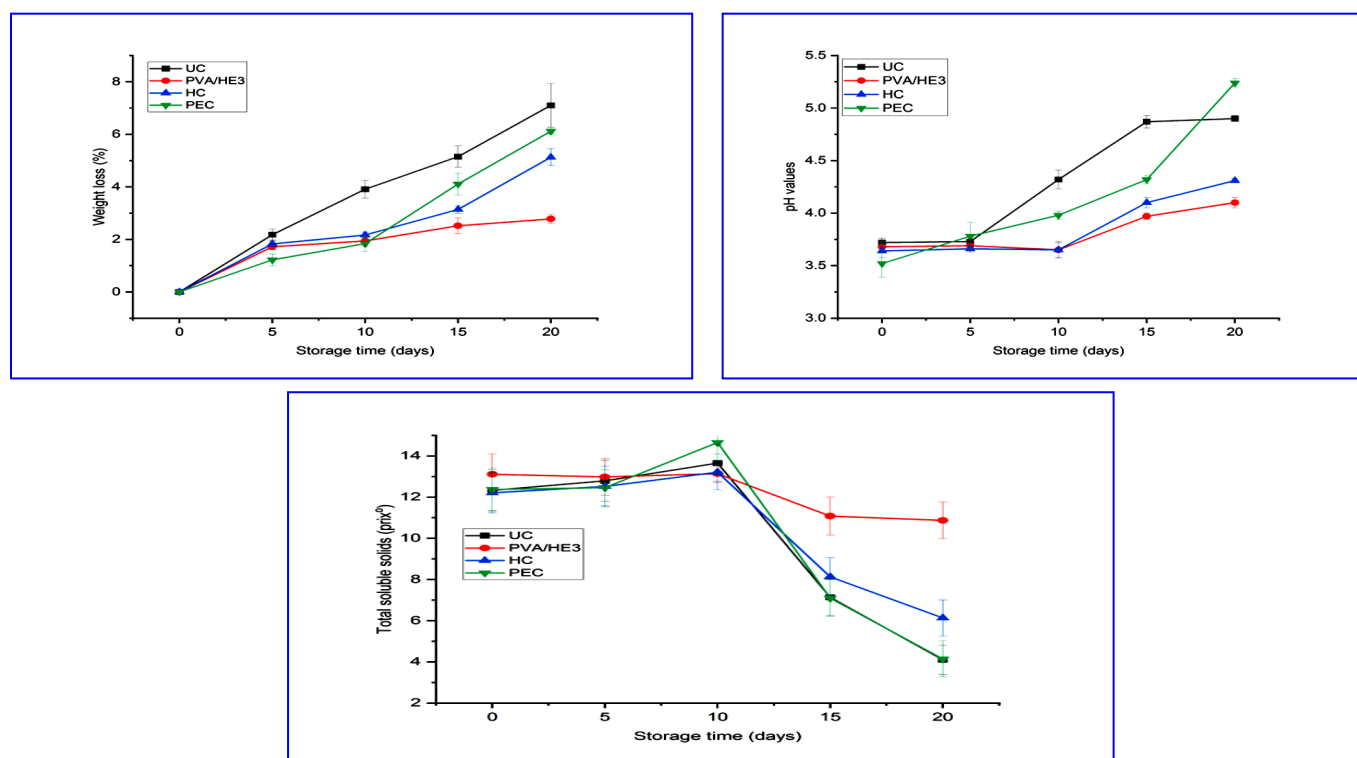


Figure 4. Antifungal activity against *Aspergillus niger* (A-C) and *Aspergillus falvus* (B-D) of PVA = films without HE and pimaricin and PVA/HE1-3 = films with stable amount from pimaricin and different concentrations from HE



**Figure 5. Effect of storage time on weight loss (A), pH values (B), total soluble solids (C) on GB fruits packaged with PVA/HE2 and PEC (poly ethylene covered) compared with UC (un coated)**

In terms of firmness (Figure 6A), it was observed that the HC fruits and GB, which were packaged with PVA/HE2, demonstrated better preservation of firmness throughout the storage period. Conversely, the UC and PEC samples experienced a significant reduction in firmness during cold storage. These findings align with the results of weight loss, indicating a correlation between firmness and weight loss. The decrease in firmness in GB can be attributed to the natural decomposition of fruit wall components caused by the activities of enzymes such as polygalacturonase,  $\beta$ -galactosidase, and pectin methylesterase. It is worth noting that fungal growth can activate these enzymes, further contributing to the reduction in firmness (Nawab et al., 2017). The preservation of firmness in PVA/HE2-coated goldenberries suggests that this treatment might retard the metabolic activity within the fruit. This, in turn, can limit gas exchange by creating a barrier with the coating (Galindez et al., 2021). Concerning reducing sugars (Fig. 6B), after 5 days of cold storage, all samples exhibited stability in terms of reducing sugar content, with no significant differences observed. However, after 5 days, all

samples showed an increase in reducing sugar content. This phenomenon can likely be attributed to the combined effects of heightened respiratory activity and the breakdown of complex polysaccharides into simpler sugars within the fruit. After 10 days of storage, there was a sharp decrease in reducing sugar content in the UC, HC, and PEC samples. This decrease may be associated with the onset of fungal growth, as fungi consume the reducing sugars present in the fruits. In contrast, the PVA/HE2-coated samples demonstrated some stability in reducing sugar content, indicating a retardation of surface fungal growth. According to (Figure 6C), the production rate of  $\text{CO}_2$  for GB fruits with different types of coatings was compared to UC samples. As expected, the UC samples exhibited the highest production rate of  $\text{CO}_2$  due to the absence of a barrier provided by the packaging used in other samples. On the other hand, the fruits packaged with PVA/HE2 showed a lower production of  $\text{CO}_2$ . This can be attributed to the well-known low permeability of PVA packaging to oxygen, which restricts gas exchange and consequently reduces the production of  $\text{CO}_2$  (Alshehri et al., 2023).

Interestingly, comparable results were reported for oranges coated with a pea starch and guar gum-

based film (Oriani et al., 2014).

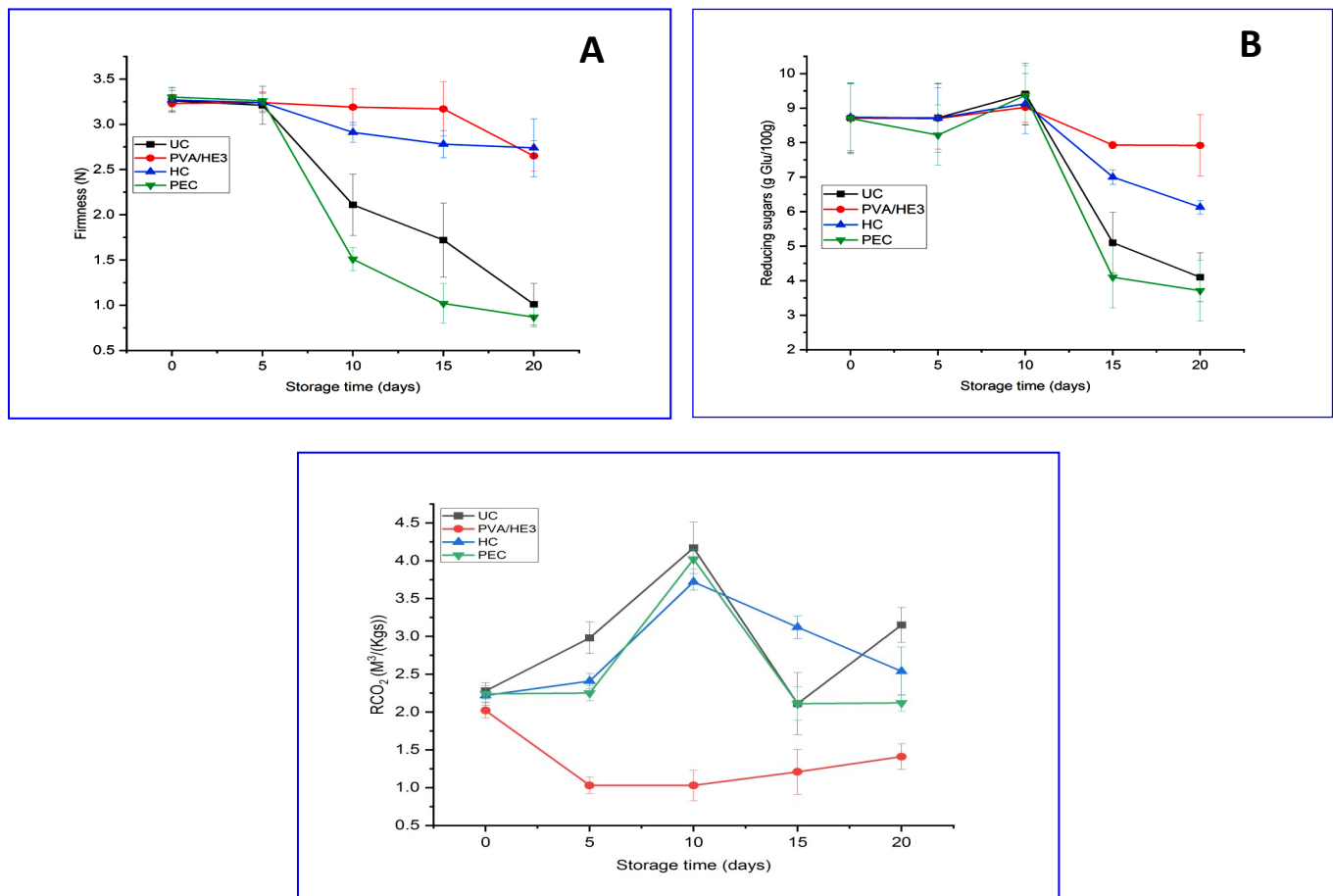


**Figure 6.** Effect of storage time on firmness (A), reducing sugars (B), respiratory rate (C) on GB fruits packaged with PVA/HE2 and PEC (poly ethylene covered) compared with UC (un coated) and HC (husk coated)

### Effect of packaging materials for GB on yeast and mold growth

During cold storage, the comparison was made between packaged goldenberries coated with PVA/HE2 and PEC, as well as UC (uncoated) and HC (husk-covered) fruits. The results in Figure 7A-B showed that the goldenberries coated with PVA/HE2 exhibited inhibition of yeast and mold growth until 15 days of cold storage. However, after 15 days, there was a slight observed growth of mold and yeast. Conversely, mold and yeast growth were observed on samples coated with PEC, HC and UC.

Figure 7C indicated that PEC-covered samples and UC samples had the highest yeast and mold growth after 20 days of cold storage. The incorporation of pimaricin and ferulic acid into the PVA/HE2 coat-

ing could potentially explain the inhibition of yeast and mold growth on the surface of goldenberries. Pimaricin is an antifungal agent that specifically binds to ergosterol in fungal cell membranes, inhibiting their growth. In contrast, ferulic acid, a phenolic compound has been shown to be metabolized by yeast and bacteria. The combination of these compounds in the PVA/HE2 packaging may contribute to the retardation of yeast and mold growth. Additionally, the regulation of respiratory rate and water vapor permeability around the fruits, facilitated by the PVA/HE2 coating, could further hinder the growth of molds and yeasts.

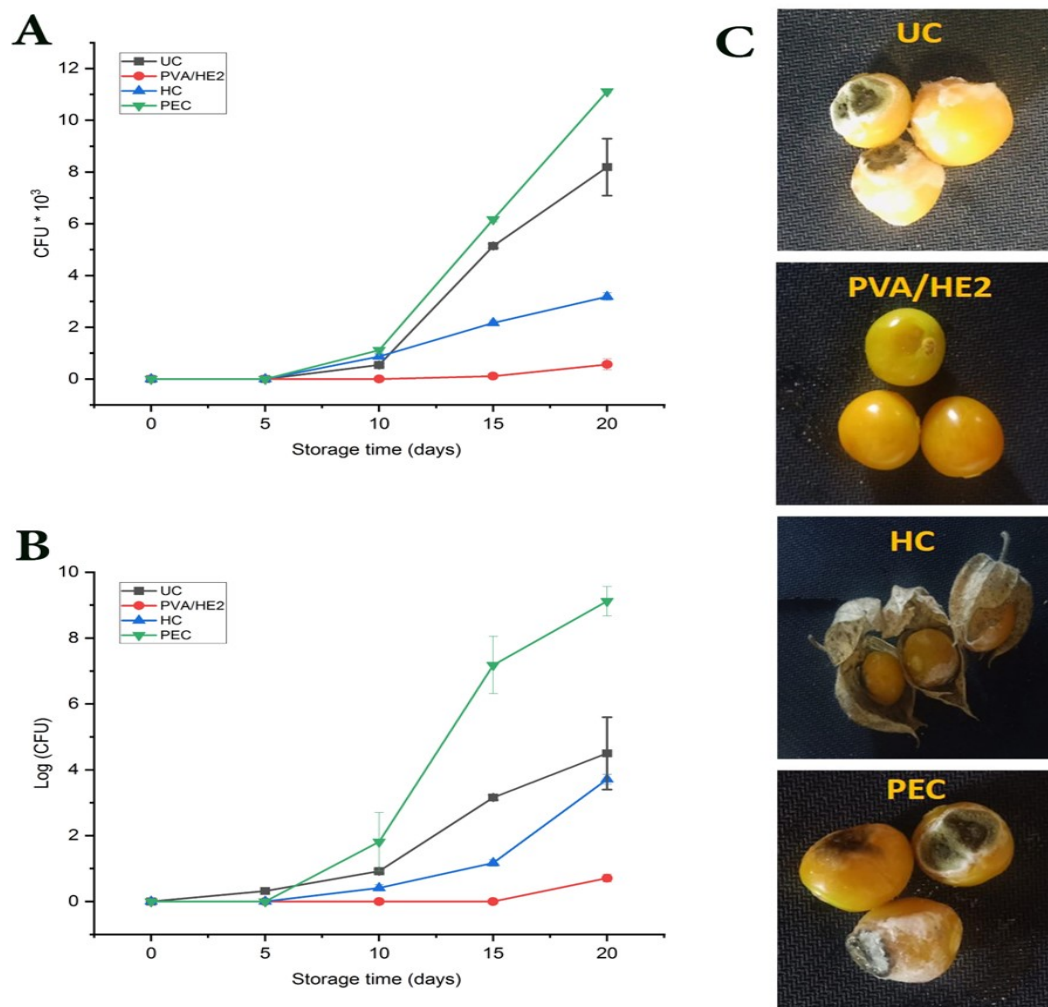


**Figure 7.** Effect of storage time on yeast (A) and molds growth (B) on GB fruits packaged with PVA/HE2 and PEC (poly ethylene covered) compared with UC (un coated) and HC (husk coated)

#### 4. Conclusion

Polyvinyl alcohol (PVA) and a hydroethanolic extract (HE) were used to create new active biocomposite films for this investigation. The presence of HE up to 0.6% inside PVA films led to a decrease in *WVP*, which suggested maintaining moderate moisture around wrapped products. Furthermore, the produced films have increased antioxidant activity, water contact angle, and antifungal activity. The prepared films were exploited to prolong the shelf life of GB fruits during cold storage. The packaging of GB with PVA/HE2 delayed the growth of yeast and molds compared with PEC, HC, and UC films. Generally, the results of the current study would pave the way for useful antifungal biodegradable films for different types of fruits.

#### Acknowledgement

The authors are most grateful for the technical support provided by the Food Technology Research Institutes, Agricultural Research Center, Giza and Sakha, Egypt.

#### References

- Abdin, M., Salama, M.A., Gawad, R., Fathi, M.A., and Alnadari, F. (2021). Two-steps of gelation system enhanced the stability of *Syzygium cumini* anthocyanins by encapsulation with sodium alginate, maltodextrin, chitosan and gum arabic. *Journal of Polymers and the Environment*, 29: 3679-3692.
- Abral, H., Atmajaya, A., Mahardika, M., Hafizulhaq, F., Handayani, D., Sapuan, S., and Ilyas, R. (2020). Effect of Ultrasonication



- duration of polyvinyl alcohol (PVA) gel on characterizations of PVA film. *Journal of Materials Research and Technology*, 9(2): 2477-2486.
- Ahmed, I., Lin, H., Zou, L., Brody, A.L., Li, Z., Qazi, I. M., Pavase, T. R., and Lv, L. (2017). A comprehensive review on the application of active packaging technologies to muscle foods. *Food Control*, 82: 163-178.
- Alnadari, F., Basse, A.P., Abdin, M., Salama, M.A., Nasiru, M.M., Dai, Z., Hu, Y., and Zeng, X. (2022). Development of hybrid film based on carboxymethyl chitosan-gum arabic incorporated citric acid and polyphenols from *Cinnamomum camphora* seeds for active food packaging. *Journal of Polymers and the Environment*, 30(9): 3582-3597.
- Alshehri, A.A., Hamed, Y.S., Kamel, R.M., Shawir, S.M., Sakr, H., Ali, M., Ammar, A., Saleh, M.N., Fadly, E. E., and Salama, M. A. (2023). Enhanced physical properties, antioxidant and antibacterial activity of bio-composite films composed from carboxymethyl cellulose and polyvinyl alcohol incorporated with broccoli sprout seed extract for butter packaging. *International Journal of Biological Macromolecules*, 128:346.
- Azhdari, S., and Moradi, M. (2022). Application of antimicrobial coating based on carboxymethyl cellulose and natamycin in active packaging of cheese. *International Journal of Biological Macromolecules*, 209: 2042-2049.
- Banda, K., Caleb, O.J., Jacobs, K., and Opara, U. L. (2015). Effect of active-modified atmosphere packaging on the respiration rate and quality of pomegranate arils (cv. Wonderful). *Postharvest Biology and Technology*, 109: 97-105.
- Cao, Y., Song, X., Xu, G., Zhang, X., Yan, H., Feng, J., Ma, Z., Liu, X., and Wang, Y. (2023). Study on the Antifungal Activity and Potential Mechanism of Natamycin against *Colletotrichum fructicola*. *Journal of agricultural and food chemistry*, 71(46): 17713-17722.
- Cazón, P., Velazquez, G., Ramírez, J.A., and Vázquez, M. (2017). Polysaccharide-based films and coatings for food packaging: A review. *Food hydrocolloids*, 68: 136-148.
- Chaudhary, B.U., Lingayat, S., Banerjee, A.N., and Kale, R.D. (2021). Development of multifunctional food packaging films based on waste Garlic peel extract and Chitosan. *International Journal of Biological Macromolecules*, 192: 479-490.
- Davachi, S.M., and Shekarabi, A.S. (2018). Preparation and characterization of antibacterial, eco-friendly edible nanocomposite films containing *Salvia macrosiphon* and nanoclay. *International Journal of Biological Macromolecules*, 113:66-72.
- Du, H., Liu, C., Unsalan, O., Altunayar-Unsalan, C., Xiong, S., Manyande, A., Chen, H., (2021). Development and characterization of fish myofibrillar protein/chitosan/rosemary extract composite edible films and the improvement of lipid oxidation stability during the grass carp fillets storage, *International journal of biological macromolecules* 184, 463-475.
- Eltabakh, M., Kassab, H., Badawy, W., Abdin, M., and Abdelhady, S. (2021). Active bio-composite sodium alginate/maltodextrin packaging films for food containing *Azolla pinnata* leaves extract as natural antioxidant. *Journal of Polymers and the Environment*, 1-11.
- Etzbach, L., Pfeiffer, A., Weber, F., and Schieber, A. (2018). Characterization of carotenoid profiles in goldenberry (*Physalis peruviana* L.) fruits at various ripening stages and in different plant tissues by HPLC-DAD-APCI-MSn. *Food chemistry*, 245: 508-517.
- Fabra, M.J., Falcó, I., Randazzo, W., Sánchez, G., and López-Rubio, A. (2018). Antiviral and antioxidant properties of active alginate edible films containing phenolic extracts. *Food hydrocolloids*, 81: 96-103.
- Fang, M., Wang, J., Fang, S., and Zuo, X. (2023). Fabrication of carboxymethyl chitosan films for cheese packaging containing gliadin-carboxymethyl chitosan nanoparticles co-encapsulating natamycin and theaflavins. *International Journal of Biological Macromolecules*, 246:125685.

- Fischer, G., Herrera, A., and Almanza, P. 2011. Cape gooseberry (*Physalis peruviana* L.). In Postharvest biology and technology of tropical and subtropical fruits, p. 374-397e Elsevier.
- Galindez, A., Daza, L. D., Homez-Jara, A., Sandoval-Aldana, A., and Váquiro, H. A. (2021). Effect of ulluco starch coating on the preservation of harvested goldenberries (*Physalis peruviana* L.). *Journal of Food Processing and Preservation*, 45(12): e16071.
- Gheorghita, R., Amariei, S., Norocel, L., and Gutt, G. (2020). New edible packaging material with function in shelf life extension: Applications for the meat and cheese industries. *Foods*, 9(5): 562.
- Gomaa, M.M., Fadly, E.E., Salama, M.A., and Abdin, M. (2022). Production of bio-composite films from gum Arabic and Galangal extract to prolong the shelf life of *Agaricus bisporus*. *Journal of Polymers and the Environment*, 30 (11):4787-4799.
- Goudarzi, J., Moshtaghi, H., and Shahbazi, Y. (2023). Kappa-carrageenan-poly (vinyl alcohol) electrospun fiber mats encapsulated with *Prunus domestica* anthocyanins and epigallocatechin gallate to monitor the freshness and enhance the shelf-life quality of minced beef meat. *Food Packaging and Shelf Life*, 35: 101017.
- Hashemi, S.M.B., Khaneghah, A.M., Ghahfarrokhi, M.G., and Eş, I. (2017). Basil-seed gum containing *Origanum vulgare* subsp. *viride* essential oil as edible coating for fresh cut apricots. *Postharvest Biology and Technology*, 125: 26-34.
- Horodytska, O., Valdés, F.J., and Fullana, A. (2018). Plastic flexible films waste management –A state of art review. *Waste management*, 77: 413-425.
- Jiang, Y., Yin, H., Zhou, X., Wang, D., Zhong, Y., Xia, Q., Deng, Y., and Zhao, Y. (2021). Antimicrobial, antioxidant and physical properties of chitosan film containing *Akebia trifoliata* (Thunb.) Koidz. peel extract/montmorillonite and its application. *Food chemistry*, 361: 130111.
- Kim, S., Baek, S.-K., and Song, K.B. (2018). Physical and antioxidant properties of alginate films prepared from *Sargassum fulvellum* with black chokeberry extract. *Food Packaging and Shelf Life*, 18: 157-163.
- Korbag, I., and Mohamed Saleh, S. (2016). Studies on the formation of intermolecular interactions and structural characterization of polyvinyl alcohol/lignin film. *International Journal of Environmental Studies*, 73(2): 226-235.
- Kraisit, P., Luangtana-Anan, M., and Sarisuta, N. (2015). Effect of Various Types of Hydroxypropyl Methylcellulose (HPMC) Films on Surface Free Energy and Contact Angle. *Advanced Materials Research*, 1060: 107-110.
- Licodiedoff, S., Koslowski, L., Scartazzini, L., Monteiro, A., Ninow, J., and Borges, C. (2016). Conservation of physalis by edible coating of gelatin and calcium chloride. *International Food Research Journal*, 23(4).
- Martins, J.T., Cerqueira, M.A., and Vicente, A.A. (2012). Influence of  $\alpha$ -tocopherol on physicochemical properties of chitosan-based films. *Food Hydrocolloids*, 27(1): 220-227.
- Meena, M., Prajapati, P., Ravichandran, C., and Sehrawat, R. (2021). Natamycin: a natural preservative for food applications—a review. *Food Science and Biotechnology*, 1-16.
- Miller, G.L. (1959). Use of dinitrosalicylic acid reagent for determination of reducing sugar. *Analytical chemistry*, 31(3): 426-428.
- Mittal, A., Singh, A., Benjakul, S., Prodpran, T., Nilsuwan, K., Huda, N., and de la Caba, K. (2021). Composite films based on chitosan and epigallocatechin gallate grafted chitosan: Characterization, antioxidant and antimicrobial activities. *Food Hydrocolloids*, 111: 106384.
- Nawab, A., Alam, F., and Hasnain, A. (2017). Mango kernel starch as a novel edible coating for enhancing shelf-life of tomato (*Solanum lycopersicum*) fruit. *International Journal of Biological Macromolecules*, 103, 581-586.
- Norajit, K., Kim, K.M., and Ryu, G.H. (2010). Comparative studies on the characterization and antioxidant properties of biodegradable alginate films containing ginseng extract. *Journal of Food Engineering*, 98(3): 377-384.

- Oriani, V.B., Molina, G., Chiumarelli, M., Pastore, G.M., and Hubinger, M.D. (2014). Properties of cassava starch-based edible coating containing essential oils. *Journal of Food Science*, 79 (2): E189-E194.
- Padgett, T., Han, I., and Dawson, P. (1998). Incorporation of food-grade antimicrobial compounds into biodegradable packaging films. *Journal of Food Protection*, 61(10): 1330-1335.
- Pankaj, S.K., Bueno-Ferrer, C., Misra, N., O'Neill, L., Tiwari, B., Bourke, P., and Cullen, P. (2014). Physicochemical characterization of plasma-treated sodium caseinate film. *Food research international*, 66: 438-444.
- Premkumar, P.S. (2019). Preparation and electrical studies on pure and oxygen plasma treated polyvinyl alcohol films. *Journal of Materials Research and Technology*, 8(2): 2232-2237.
- Severo, C., Anjos, I., Souza, V.G., Canejo, J.P., Bronze, M., Fernando, A.L., Coelho, I., Bettencourt, A.F., and Ribeiro, I.A. (2021). Development of cranberry extract films for the enhancement of food packaging antimicrobial properties. *Food Packaging and Shelf Life*, 28: 100646.
- Siripatrawan, U., and Harte, B.R. (2010). Physical properties and antioxidant activity of an active film from chitosan incorporated with green tea extract. *Food hydrocolloids*, 24(8): 770-775.
- Sogut, E., and Seydim, A.C. (2018). The effects of Chitosan and grape seed extract-based edible films on the quality of vacuum packaged chicken breast fillets. *Food Packaging and Shelf Life*, 18: 13-20.
- Su, J.-F., Huang, Z., Yuan, X.-Y., Wang, X.-Y., and Li, M. (2010). Structure and properties of carboxymethyl cellulose/soy protein isolate blend edible films crosslinked by Maillard reactions. *Carbohydrate Polymers*, 79(1): 145-153.
- Talukder, S., Mendiratta, S., Kumar, R., Agrawal, R., Soni, A., Luke, A., and Chand, S. (2020). Jamun fruit (*Syzygium cumini*) skin extract based indicator for monitoring chicken patties quality during storage. *Journal of food science and technology*, 57:537-548.
- Thakur, R., Pristijono, P., Bowyer, M., Singh, S.P., Scarlett, C.J., Stathopoulos, C.E., and Vuong, Q.V. (2019). A starch edible surface coating delays banana fruit ripening. *Lwt*, 100: 341-347.
- Thakur, R., Pristijono, P., Golding, J., Stathopoulos, C.E., Scarlett, C., Bowyer, M., Singh, S., and Vuong, Q. (2018). Development and application of rice starch based edible coating to improve the postharvest storage potential and quality of plum fruit (*Prunus salicina*). *Scientia Horticulturae*, 237: 59-66.
- Xu, X., Peng, X., Huan, C., Chen, J., Meng, Y., and Fang, S. (2023). Development of natamycin-loaded zein-casein composite nanoparticles by a ph-driven method and application to postharvest fungal control on peach against *Monilinia fructicola*. *Food chemistry*, 404: 134659.
- Yan, H., Meng, X., Lin, X., Duan, N., Wang, Z., and Wu, S. (2023). Antifungal activity and inhibitory mechanisms of ferulic acid against the growth of *Fusarium graminearum*. *Food Bioscience*, 52: 102414.
- Yao, X., Hu, H., Qin, Y., and Liu, J. (2020). Development of antioxidant, antimicrobial and ammonia-sensitive films based on quaternary ammonium chitosan, polyvinyl alcohol and betalains-rich cactus pears (*Opuntia ficus-indica*) extract. *Food hydrocolloids*, 106: 105896.
- Zarandona, I., Puertas, A., Dueñas, M., Guerrero, P., and De La Caba, K. (2020). Assessment of active chitosan films incorporated with gallic acid. *Food Hydrocolloids*, 101: 105486.